

## Value of intravoxel incoherent motion in detecting and staging liver fibrosis: A meta-analysis

Zheng Ye, Yi Wei, Jie Chen, Shan Yao, Bin Song

**ORCID number:** Zheng Ye (0000-0001-6715-0183); Yi Wei (0000-0003-3993-9747); Jie Chen (0000-0002-7543-0449); Shan Yao (0000-0002-0665-2566); Bin Song (0000-0001-9227-8584).

**Author contributions:** Ye Z contributed to the conception and design of the study, carried out acquisition, analysis, and interpretation of data, and drafted the article; Wei Y and Chen J interpreted the data and revised the article; Yao S carried out acquisition, analysis, and interpretation of data; Song B contributed to the conception and design of the study and final approval; All authors approved the final version of the article.

**Supported by** the National Nature Science Foundation of China, No. 81771797 and No. 81971571; and the 1.3.5 Project for Disciplines of Excellence, West China Hospital, Sichuan University, No. ZYJC18008.

**Conflict-of-interest statement:** The authors have no conflicts of interest to declare.

**PRISMA 2009 Checklist statement:** The authors have read the PRISMA 2009 Checklist, and the manuscript was prepared and revised according to the PRISMA 2009 Checklist.

**Open-Access:** This article is an open-access article that was selected by an in-house editor and fully peer-reviewed by external reviewers. It is distributed in accordance with the Creative Commons Attribution

**Zheng Ye, Yi Wei, Jie Chen, Shan Yao,** West China School of Medicine, Sichuan University, Chengdu 610041, Sichuan Province, China

**Bin Song,** Department of Radiology, West China Hospital, Sichuan University, Chengdu 610041, Sichuan Province, China

**Corresponding author:** Bin Song, PhD, Chief Doctor, Department of Radiology, West China Hospital, Sichuan University, No. 37 Guoxue Alley, Chengdu 610041, Sichuan Province, China. [songb\\_radiology@163.com](mailto:songb_radiology@163.com)

### Abstract

#### BACKGROUND

Liver fibrosis (LF) is a common pathological feature of all chronic liver diseases. With the accumulation of extracellular matrix in the fibrotic liver, true molecular water diffusion and perfusion-related diffusion are restricted. Intravoxel incoherent motion (IVIM) can capture the information on tissue diffusivity and microcapillary perfusion separately and reflect the fibrotic severity with diffusion coefficients.

#### AIM

To investigate the diagnostic performance of IVIM in detecting and staging LF with histology as a reference standard.

#### METHODS

A comprehensive literature search was conducted to identify studies on the diagnostic accuracy of IVIM for assessment of histologically proven LF. The stages of LF were classified as F0 (no fibrosis), F1 (portal fibrosis without septa), F2 (periportal fibrosis with few septa), F3 (septal fibrosis), and F4 (cirrhosis) according to histopathological findings. Data were extracted to calculate the pooled sensitivity, specificity, positive and negative likelihood ratios, and diagnostic odds ratio, as well as the area under the summary receiver operating characteristic curve (AUC) in each group.

#### RESULTS

A total of 12 studies with 923 subjects were included in this meta-analysis with 5 studies ( $n = 465$ ) for LF  $\geq$  F1, 9 studies ( $n = 757$ ) for LF  $\geq$  F2, 4 studies ( $n = 413$ ) for LF  $\geq$  F3, and 6 studies ( $n = 562$ ) for LF = F4. The pooled sensitivity and specificity were estimated to be 0.78 (95% confidence interval: 0.73-0.82) and 0.81 (0.74-0.86) for LF  $\geq$  F1 detection with IVIM; 0.82 (0.79-0.86) and 0.80 (0.75-0.84) for staging F2 fibrosis; 0.85 (0.79-0.90) and 0.83 (0.77-0.87) for staging F3 fibrosis, and 0.90 (0.84-0.94) and 0.75 (0.70-0.79) for detecting F4 cirrhosis, respectively. The AUCs for LF

NonCommercial (CC BY-NC 4.0) license, which permits others to distribute, remix, adapt, build upon this work non-commercially, and license their derivative works on different terms, provided the original work is properly cited and the use is non-commercial. See: <http://creativecommons.org/licenses/by-nc/4.0/>

**Manuscript source:** Invited manuscript

**Received:** December 30, 2019

**Peer-review started:** December 30, 2019

**First decision:** February 18, 2020

**Revised:** March 26, 2020

**Accepted:** May 29, 2020

**Article in press:** May 29, 2020

**Published online:** June 21, 2020

**P-Reviewer:** Yong D

**S-Editor:** Dou Y

**L-Editor:** Filipodia

**E-Editor:** Ma YJ



≥ F1, F2, F3, F4 detection were 0.862 (0.811-0.914), 0.883 (0.856-0.909), 0.886 (0.865-0.907), and 0.899 (0.866-0.932), respectively. Moderate to substantial heterogeneity was observed with inconsistency index ( $I^2$ ) ranging from 0% to 77.9%. No publication bias was detected.

### CONCLUSION

IVIM is a noninvasive tool with good diagnostic performance in detecting and staging LF. Optimized and standardized IVIM protocols are needed to further improve its diagnostic accuracy in clinical practice.

**Key words:** Liver fibrosis; Liver cirrhosis; Intravoxel incoherent motion; Diffusion weight imaging; Diffusion magnetic resonance imaging; Meta-analysis

©The Author(s) 2020. Published by Baishideng Publishing Group Inc. All rights reserved.

**Core tip:** Intravoxel incoherent motion (IVIM) can separately evaluate the change of true molecular diffusion and perfusion-related diffusion caused by liver fibrosis (LF). This is the first meta-analysis to investigate the performance of IVIM for LF detection and staging with comprehensive diagnostic estimates. The results showed that IVIM is a valuable tool in noninvasively detecting and staging LF. However, field strength, the number and distribution of b-values, as well as the triggering methods affect the diagnostic accuracy. There is still a need to establish an optimized and standardized IVIM protocol for LF diagnosis in clinical practice.

**Citation:** Ye Z, Wei Y, Chen J, Yao S, Song B. Value of intravoxel incoherent motion in detecting and staging liver fibrosis: A meta-analysis. *World J Gastroenterol* 2020; 26(23): 3304-3317

**URL:** <https://www.wjgnet.com/1007-9327/full/v26/i23/3304.htm>

**DOI:** <https://dx.doi.org/10.3748/wjg.v26.i23.3304>

## INTRODUCTION

Liver fibrosis (LF) is characterized by the excessive accumulation of extracellular matrix (primarily collagen type I)<sup>[1]</sup>. It is a common pathological feature of chronic liver disease caused by various etiologies, which may progress to hepatic dysfunction, portal hypertension, and even hepatocellular carcinoma, resulting in increased morbidity and mortality<sup>[2]</sup>. Early or intermediate LF is considered to be reversible with timely medical intervention and anti-fibrotic treatments<sup>[3]</sup>. Hence, early detection and accurate staging of LF is of great clinical significance in making appropriate therapeutic decisions and evaluating patient prognosis.

Liver biopsy is the current reference standard in detecting and staging LF. According to histologic scoring systems, the spectrum of fibrosis severity can be divided into several stages, for example, semi-quantitatively scoring as F0 (no fibrosis), F1 (portal fibrosis without septa), F2 (periportal fibrosis with few septa), F3 (septal fibrosis) and F4 (cirrhosis) in the METAVIR system<sup>[4]</sup>. However, liver biopsy is invasive, observer-dependent, and prone to sampling variability<sup>[5]</sup>, all which hampers its widespread use in clinical practice; thus, a noninvasive method to quantify LF is urgently needed. Recently, magnetic resonance imaging (MRI) techniques have been increasingly applied to LF detection and staging and could possibly be a noninvasive alternative to liver biopsy<sup>[6]</sup>.

Diffusion-weighted imaging (DWI) can capture the information of Brownian motion (random motion of water molecules) and quantitatively reflect the degrees of extracellular matrix accumulation *via* apparent diffusion coefficient (ADC), which has been previously reported as a good diagnostic tool in LF<sup>[7-9]</sup>. However, the diffusion process would be mimicked and confounded by the blood flow in capillaries (perfusion process), thereby affecting diffusion MRI measurements<sup>[10]</sup>. Intravoxel incoherent motion (IVIM), a bi-exponential model based on DWI, allows for the separate evaluation of true molecular diffusion and perfusion-related diffusion, which is more informative than DWI<sup>[10,11]</sup>. Although several recent studies focused on the diagnostic performances of IVIM in LF staging, there were discrepancies in the reported results among studies<sup>[12-15]</sup>. In 2016, Zhang *et al*<sup>[16]</sup> conducted a meta-analysis

on this topic; however, due to the limited number of included studies, they only performed pooled weighted mean difference to compare the difference of IVIM parameters among LF stages, and failed to conclude the pooled diagnostic indexes to comprehensively evaluate the value of IVIM in detecting and staging LF.

Therefore, with more eligible studies and patients included, the purpose of this meta-analysis was to investigate the diagnostic performance of IVIM in different LF stages with histology as reference.

## MATERIALS AND METHODS

### Literature search

Two independent investigators conducted a comprehensive literature search of the Cochrane Library, Ovid MEDLINE, Web of Science, EMBASE and Google Scholar databases to identify relevant publications (literature retrieval until December 2019). The following keywords and search strategy were used: “IVIM OR intravoxel incoherent motion OR biexponential DWI OR diffusion magnetic resonance imaging” AND “liver/hepatic fibrosis OR liver/hepatic cirrhosis.” The search was limited to articles in the English language.

### Inclusion and exclusion criteria

The inclusion criteria were as follows: (1) IVIM was performed for LF detection and staging; (2) Hepatic histological analysis was used as the reference standard for all LF patients; and (3) Sufficient data were provided to calculate the values of true-positive (TP), false-positive (FP), false-negative (FN), and true-negative (TN). The studies were excluded if they were: (1) Reviews, letters, editorials, comments, case reports, or guidelines; (2) Duplicate publications; and (3) *ex vivo*, phantom, or animal research.

### Data extraction and quality assessment

The following information were extracted from each study: author, publication year, country, study design (prospectively or retrospectively), study population, patient baseline characteristics (sex ratio, mean age, disease spectrum), reference standard, histopathological characteristics, blinding procedure, detailed MRI protocol (scanner, field strength, trigger methods, b-values, scan time) and time intervals between MRI examination and reference test. Meanwhile, the best diagnostic parameter and its diagnostic threshold as well as TP, FP, FN, TN were recorded. For detecting and staging LF, we respectively extracted diagnostic data and  $2 \times 2$  contingency tables in four subgroups, which were LF  $\geq$  F1 (F0 vs F1-F4, detecting LF from normal liver), LF  $\geq$  F2 (F0-F1 vs F2-F4, differentiating moderate LF), LF  $\geq$  F3 (F0-F2 vs F3-F4, differentiating severe LF) and LF = F4 (F0-F3 vs F4, detecting liver cirrhosis). The Quality Assessment of Diagnostic Accuracy Studies (QUADAS-2) scale<sup>[17]</sup> was used to evaluate the quality of included studies. The other two investigators independently performed data extraction and quality assessment and reached to consensus by discussion or by consulting a senior abdominal radiologist if opinions differed.

### Statistical analysis

The pooled sensitivities, specificities, positive likelihood ratio, negative likelihood ratio and diagnostic odds ratio with corresponding 95% confidence interval (CI) were calculated by using random-effects coefficient binary regression model<sup>[18]</sup>. The summary receiver operating characteristic (SROC) curves analysis were constructed in each LF group, and the areas under the curves (AUCs) were also calculated<sup>[19]</sup>. Heterogeneity among included studies was evaluated by using Q statistic of the  $\chi^2$  test and the inconsistency index ( $I^2$ ), with  $I^2 = 25\%$ - $50\%$  indicating low heterogeneity,  $I^2 = 51\%$ - $75\%$  indicating moderate heterogeneity and  $I^2 > 75\%$  indicating substantial heterogeneity<sup>[20]</sup>. To explore the potential sources of heterogeneity, the threshold effect was firstly examined by computing Spearman correlation coefficient between the logit of sensitivity and the logit of (1-specificity), and a significant strong positive correlation ( $P < 0.05$ ) would suggest the presence of threshold effect<sup>[21]</sup>. Meta regression or subgroup analysis (depending on the number of included studies) was performed to find the possible sources other than threshold effect of heterogeneity<sup>[22]</sup>. Sensitivity analyses were also conducted to evaluate the stability and reliability of the summary results. To evaluate potential publication bias of the included studies, Deeks' funnel plot asymmetry test was conducted, and a P value higher than 0.05 in linear regression test indicated that there was no publication bias<sup>[23]</sup>. All statistical analyses were performed using Meta-Disc (version 1.4), Stata (version 12.0) and Reviewer Manager (version 5.3).

## RESULTS

### Literature search

A total of 890 studies were initially identified in the databases. After removing the duplicates, the remaining 655 studies were assessed by title, abstract and full paper. Finally, 12 studies with 923 subjects were included in this meta-analysis. The flowchart of studies inclusion and exclusion are shown in [Figure 1](#).

### Study characteristics and quality assessment

The baseline, methodological, and imaging protocol characteristics of the included studies are shown in [Table 1](#) and [Table 2](#). Of these 12 studies, there were 5 studies ( $n = 465$ ) for  $LF \geq F1$ <sup>[24-28]</sup>, 9 studies ( $n = 757$ ) for  $LF \geq F2$ <sup>[25-27,29-34]</sup>, 4 studies ( $n = 413$ ) for  $LF \geq F3$ <sup>[25-27,35]</sup> and 6 studies ( $n = 562$ ) for  $LF = F4$ <sup>[25-27,29,31,33]</sup>. The best IVIM index, diagnostic threshold as well as reporting TP, FP, FN, TN, sensitivity and specificity in four LF groups were displayed in [Table 3](#). The quality of included studies was good according to the QUADAS-2 scale ([Figure 2](#)).

### Pooled diagnostic performance

The summarized diagnostic estimates are shown in [Table 4](#). Pooled sensitivities and pooled specificities were estimated to be 0.78 (0.73-0.82) and 0.81 (0.74-0.86) for  $LF \geq F1$ , 0.82 (0.79-0.86) and 0.80 (0.75-0.84) for  $LF \geq F2$ , 0.85(0.79-0.90) and 0.83 (0.77-0.87) for  $LF \geq F3$ , and 0.90 (0.84-0.94) and 0.75 (0.70-0.79) for  $LF = F4$ , respectively. According to SROC analysis, the AUCs were 0.862 (0.811-0.914), 0.883 (0.856-0.909), 0.886 (0.865-0.907) and 0.899 (0.866-0.932) for  $LF \geq F1$ ,  $F2$ ,  $F3$  and  $F4$ , respectively. SROC curves of four LF groups are demonstrated in [Figure 3](#). Forest plots of sensitivity and specificity are shown [Supplementary materials part 1](#).

### Assessment of heterogeneity

There were moderate to substantial heterogeneity in our meta-analysis with  $I^2$  ranging from 0% to 77.9% in pooled sensitivity and pooled specificity [Supplementary materials part 1](#) (materials part 1). Threshold effect was eliminated by visual assessment of ROC plane, which showed no evidence of "shoulder-arm" shape, and the Spearman correlation coefficient, reporting 0.10 ( $P = 0.87$ ), 0.47 ( $P = 0.21$ ), -0.20 ( $P = 0.80$ ) and 0.66 ( $P = 0.16$ ) for  $LF \geq F1$ ,  $F2$ ,  $F3$  and  $F4$ , respectively. According to Cochrane handbook, meta regression was generally not considered when there were fewer than ten studies, so we conducted subgroup analysis to explore the potential contributors of heterogeneity in  $LF \geq F2$  group. The eligible studies for  $LF \geq F1$ ,  $F3$  and  $F4$  were too limited to perform meta-regression and subgroup analysis, and thus sensitivity analyses were conducted to test the robustness of results, which suggested our results were reliable ([Supplementary materials part 2](#)).

### Subgroup analysis

We performed subgroup analysis to evaluate the possible sources of heterogeneity in  $LF \geq F2$  group in terms of study design, blindness manner, field strength, number of low b-values and IVIM trigger methods. The retrospective and double-blinded studies showed slightly higher AUC than prospective and unclear blinded studies. And the AUCs of studies using 3.0 T, more low-b-values and non-respiratory-triggered (RT) IVIM protocol were higher than those of studies with 1.5 T, less low-b-values and RT protocol. The detailed results of subgroup analysis are shown in [Table 4](#).

### Publication bias

The  $P$  values in Deeks' tests were 0.18 for  $LF \geq F1$ , 0.28 for  $LF \geq F2$ , and 0.20 for  $LF \geq F3$ , and 0.84 for  $LF = F4$ , respectively, which suggested the absence of notable publication bias ([Supplementary materials part 3](#)).

## DISCUSSION

With the accumulation of extracellular matrix (especially the collagen) in the fibrotic liver, the molecular water diffusion would be restricted, and the changes of fibrosis severity would be reflected in the diffusion parameters<sup>[36,37]</sup>. However, due to the relatively high hepatic blood volume fraction, perfusion-related diffusion, which was caused by incoherent motion of blood in pseudorandom capillary network, can contribute significantly to the true diffusion measurements, thus affecting the accuracy of traditional ADC in DWI<sup>[13]</sup>. Therefore, Le Bihan *et al*<sup>[10]</sup> proposed IVIM theory to capture the information of tissue diffusivity and microcapillary perfusion separately. In this meta-analysis, we included 12 eligible studies, and summarized the results based on a systematic and extensive statistical analysis, providing the pooled

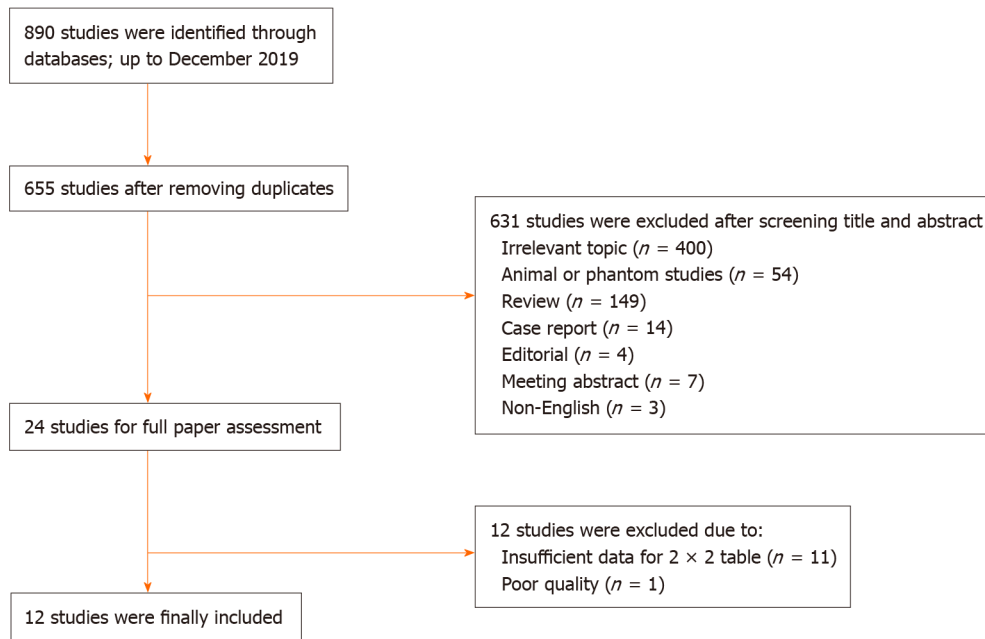


Figure 1 Flowchart of study inclusion and exclusion.

diagnostic estimates to simulate a large sample study and trying to overcome the limitations that previous studies have mentioned. According to our results, IVIM showed good but not perfect diagnostic accuracy in detecting and staging LF with AUCs ranging from 0.862 (0.811-0.914) to 0.899 (0.866-0.932).

There are three diagnostic parameters in IVIM model:  $S_b/S_0 = (1-f) \exp(-bD_t) + f \exp[-b(D_t + D^*)]$ .

Where  $D_t$  is true diffusion coefficient, which was free from perfusion effects;  $D^*$  is pseudo-diffusion coefficient or perfusion-related diffusion and  $f$  stands for the fraction of the perfusion component<sup>[11]</sup>. In most studies,  $D^*$  was reported to decrease significantly with the progression of LF and considered as the best diagnostic parameter in detecting and staging LF, probably because of the architectural disruption and underlying hemodynamics changes of arterial and portal blood flow in fibrotic liver<sup>[29,38]</sup>. However, in this meta-analysis, there were one or two studies suggesting  $D_t$  or  $f$  as the best diagnostic index in each LF group<sup>[25,34,35]</sup>, as demonstrated in Table 3, which may be attributed to the different  $b$  value distributions in those studies and the relatively large variability of  $D^*$ <sup>[39]</sup>. Although we have validated good reliability of our results by conducting sensitivity analyses in terms of different diagnostic parameters, further investigations are needed to explore the optimal IVIM parameter and its threshold in LF detection and staging.

LF  $\geq$  F2 is considered as the clinically significant fibrosis and is a crucial time point for anti-fibrotic treatment<sup>[3]</sup>. In this meta-analysis, substantial heterogeneity was detected in LF  $\geq$  F2 group; therefore we performed subgroup analyses to explore the possible contributors. To our knowledge, there is no clear consensus on the number and distribution of  $b$ -values in IVIM protocol so far. Theoretically, four  $b$ -values would be sufficient for fitting a biexponential model; however, including more  $b$ -values would provide added robustness to the fit process, and low  $b$ -values is particularly important in fitting pseudo-diffusion constant<sup>[40]</sup>. In subgroup analysis, our results revealed that including three or more low  $b$ -values ( $0 < b < 50$  s/mm<sup>2</sup>) would obtain a slightly higher diagnostic performance in detecting F2 fibrosis (AUC: 0.877 vs 0.890), which were in accordance with Cohen *et al*<sup>[41]</sup> who recommended including at least two low  $b$ -values to ensure the accuracy when conducting liver IVIM research. Previous studies have tried to figure out the optimized  $b$ -values number and distribution in different clinical scenarios, however, the conclusions varied in those studies<sup>[42,43]</sup>, and investigators have to balance the parameter estimation quality with the acquisition time during this process.

Apart from  $b$ -values, IVIM triggering methods is another key factor in acquisition time. Typically, scanning time of free-breathing (FB) IVIM is predetermined and often less than 5 min, while the time of RT IVIM is unpredictable, usually longer (5-10 min) and highly depends on subjects' respiratory condition<sup>[44]</sup>. It is known that the RT

Table 1 Baseline characteristics of the included studies and subjects

Ref.	Year	Country	Study design	Sample size	Sex ratio, M/F	mean $\pm$ SD age in yr	Patient spectrum (n)
Yoon <i>et al</i> <sup>[30]</sup>	2019	South Korea	Retro	106	81/25	55.4 $\pm$ 11.6	HBV (82), HCV (9), non-B non-C cirrhosis (3), ALD (10), PBC (2)
Fu <i>et al</i> <sup>[25]</sup>	2019	China	Pros	125	71/54	37.6 $\pm$ 9.3 (patients), 31.5 $\pm$ 12.9 (volunteers)	HBV (81), HCV (8), NAFLD (3), DIH (2), AIH (6)
Zawada <i>et al</i> <sup>[34]</sup>	2019	Poland	Pros	40	10/30	22-75	HCV (40)
Sandrasegaran <i>et al</i> <sup>[32]</sup>	2018	United States	Retro	49	35/14	56.6 (range: 32-73)	HBV (3), HCV (35), ALD (24), AIH (4), Other (7) <sup>1</sup>
Seo <i>et al</i> <sup>[31]</sup>	2018	South Korea	Retro	95	70/25	59.5 $\pm$ 9.5	HBV (44), HCV (7), ALD (14), no underlying liver disease (30)
Hu <i>et al</i> <sup>[29]</sup>	2017	China	Retro	56	14/42	47.48 (range: 15-76)	HBV (5), NAFLD (14), ASH (1), PSC (8), AIH (10), overlap syndrome of AIH (5), and DIH (13)
Chung <i>et al</i> <sup>[35]</sup>	2015	South Korea	Retro	57	35/22	58.7 (range: 32-89)	HBV (34), HCV (1), ALD (2), Other (20)
Wu <i>et al</i> <sup>[27]</sup>	2015	China (Taiwan)	Pros	49	36/13	62.4 (range: 38-85)	HBV (17), HVC (10), non-B non-C carriers (17), both hepatitis B and C carriers (5)
Ichikawa <i>et al</i> <sup>[26]</sup>	2015	Japan	Retro	182	127/55	66.4 $\pm$ 11.6	HBV (18), HCV (62), ASH (12), NASH (3), AIH (1), PBC (2), unidentified liver disease with an elevated liver enzyme level (12)
Parente <i>et al</i> <sup>[28]</sup>	2015	Brazil	Pros	59	10/49	54 $\pm$ 9	Type 2 diabetic subjects (59)
Chen <i>et al</i> <sup>[24]</sup>	2014	China	Pros	50	37/13	43.7 $\pm$ 1.2 (patients), 38.9 $\pm$ 1.3 (volunteers)	HBV (15), HCV (1), ALD (1), unidentified liver disease with an elevated liver enzyme level (8)
Yoon <i>et al</i> <sup>[33]</sup>	2014	South Korea	Retro	55	42/13	53.9 (range: 18-78)	HBV (45), HCV (1), ALD (1), Other (8)

<sup>1</sup>Some patients had more than one etiology of liver disease. M/F: Male/female; SD: Standard deviation; Retro: Retrospective; Pros: Prospective; HBV: Hepatitis B virus; HCV: Hepatitis C virus; ALD: Alcoholic liver disease; PBC: Primary biliary cirrhosis; PSC: Primary sclerotic cholangitis; NAFLD: Nonalcoholic fatty liver disease; NASH: Nonalcoholic steatohepatitis; DIH: Drug-induced hepatitis; AIH: Autoimmune hepatitis; ASH: Alcoholic steatohepatitis.

technique enables the reduction of motion-related blurring by tracking the movement from the respiratory cycle and acquiring data only in the same phase; however, patients' irregular breathing can decrease the time-efficiency of the acquisition or, in some cases, make the navigator tracking unusable<sup>[45,46]</sup>. In our study, results of subgroup analysis showed that diagnostic performance of IVIM was lower in five studies with RT method, compared with four studies with non-RT (FB or unclear) method (AUC: 0.867 *vs* 0.919). Although still controversial, our findings together with most previous studies indicated that RT method offers no advantage in fitting IVIM parameters and could be substituted by FB method, which is usually more comfortable for the patients<sup>[45-47]</sup>. In addition, Riexinger *et al*<sup>[48]</sup> recently found that

**Table 2** Methodological and imaging protocol characteristics of included studies

Ref.	Reference standard	Scoring system	F0/F1/F2/F3/F4	Mean intervals	Double blindness	Scanner	FS	Trigger methods	b values	Scan time <sup>1</sup>
Yoon <i>et al</i> <sup>[30]</sup> , 2019	S/B	METAVIR	13/6/19/18/50	6 (4-38) d	Yes	GE	1.5 T	FB	0, 15, 25.4, 42.9, 72.5, 122.5, 207, 350, 592, 1000	4.5
Fu <i>et al</i> <sup>[25]</sup> , 2019	S/B	METAVIR	26/17/33/25/24	< 1 mo	Yes	GE	3.0 T	RT	0, 50, 100, 150, 200, 300, 500, 800, 1000, 1300, 1500, 1700, 2000	10
Zawada <i>et al</i> <sup>[34]</sup> , 2019	B	Scheuer scale	7/17/10/2/2	NA	Unclear	GE	1.5 T	RT	0, 20, 50, 100, 200, 400, 600, 800, 1000	2.6
Sandrasegaran <i>et al</i> <sup>[32]</sup> , 2018	B	METAVIR	4/8/2/9/26	< 3 mo	Unclear	Siemens	1.5 T	RT	0, 50, 100, 300, 600, 800	12-15
Seo <i>et al</i> <sup>[31]</sup> , 2018	S/B/T	Batts-Ludwig	30/14/4/18/29	81.2 d	Yes	Philips	3.0 T	FB	0, 10, 25, 50, 75, 100, 200, 500, 800	4.25
Hu <i>et al</i> <sup>[29]</sup> , 2017	B	METAVIR	6/19/13/8/10	6 d	Unclear	Siemens	3.0 T	NA	0, 25, 50, 75, 100, 150, 200, 500, 800	5
Chung <i>et al</i> <sup>[35]</sup> , 2015	B/I	METAVIR	21/1/6/7/22	15.9 (2-43) d	Unclear	Siemens	1.5 T	RT	0, 30, 60, 100, 150, 200, 400, 600, 900	7
Wu <i>et al</i> <sup>[27]</sup> , 2015	S	METAVIR	6/16/10/10/7	< 7 d	Unclear	Siemens	3.0 T	RT	0, 10, 20, 30, 40, 50, 60, 70, 80, 90, 100, 200, 300, 400, 500, 1000	< 7
Ichikawa <i>et al</i> <sup>[26]</sup> , 2015	S/B	METAVIR	72/13/14/19/64	< 3 mo	Unclear	GE	3.0 T	RT	0, 10, 20, 30, 40, 50, 80, 100, 200, 500, 1000	2-3
Parente <i>et al</i> <sup>[28]</sup> , 2015	B	METAVIR	43/9/5/1/1	< 3 mo	Unclear	Philips	3.0 T	RT	0, 10, 20, 40, 80, 160, 200, 400, 800, 1000	3
Chen <i>et al</i> <sup>[24]</sup> , 2014	B	METAVIR	25/4/9/11/1	< 1 mo	Unclear	GE	3.0 T	RT	0, 50, 100, 200, 400, 600, 800	NA
Yoon <i>et al</i> <sup>[33]</sup> , 2014	S/B/T	METAVIR	11/7/7/9/21	NA	Unclear	Siemens	3.0 T	FB	0, 25, 50, 75, 100, 200, 500, 800	6.5

<sup>1</sup>The unit of scan time is min. NA: Not available; S: Liver surgery; B: Percutaneous liver biopsy; T: Liver transplantation; I: Imaging findings; FS: Field strength; FB: Free breathing; RT: Respiratory triggered.

IVIM parameters of the liver showed a significant dependency on the applied field strength, hence we also conducted subgroup analysis in this regard. Commonly speaking, 3.0 T is much more sensitive to magnetic susceptibility induced artifacts and eddy current related distortion<sup>[37]</sup>, however, our results indicated higher diagnostic performance of IVIM in 3.0 T scanners with AUC of 0.904, compared with 1.5 T scanners with AUC of 0.839. Cui *et al*<sup>[49]</sup> also reported the similar findings and concluded the improved signal-to-noise ratio in high field strength may be the underlying reason. Therefore, the standardized and optimized IVIM protocols in different field strength should be investigated in the future for better clinical practice.

Other sophisticated diffusion models were also considered feasible in detecting and staging LF, including diffusion kurtosis imaging (DKI)<sup>[50]</sup>, diffusion tensor imaging (DTI)<sup>[51]</sup>, tri-exponential IVIM model<sup>[52]</sup> and stretched exponential model<sup>[53]</sup>. However, except for the stretched exponential model, other diffusion models showed no added

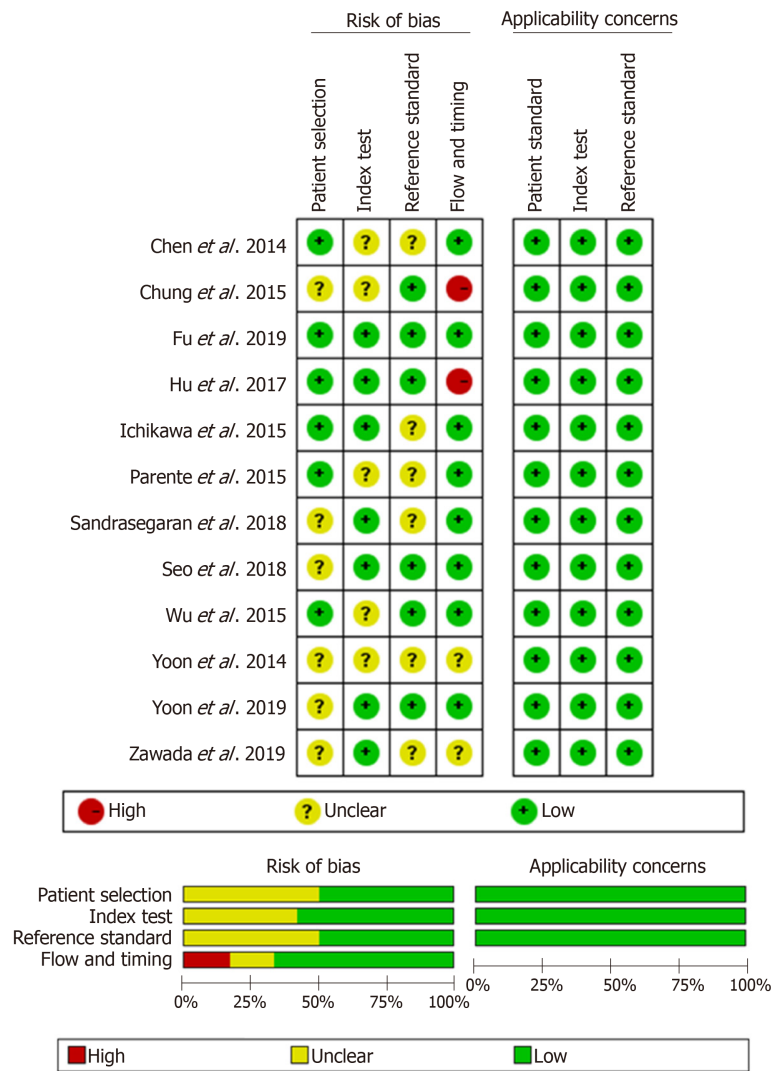


**Figure 2** Quality assessment of included studies according to Quality Assessment of Diagnostic Accuracy Studies-2. The results showed that the quality of the included studies was good.

diagnostic value to conventional DWI or bi-exponential IVIM for LF detection and staging<sup>[50-52]</sup>. Recently, Seo *et al.*<sup>[31]</sup> and Fu *et al.*<sup>[25]</sup> both reported the higher diagnostic potential of distributed diffusion coefficient (DDC) in stretched exponential model, compared with DWI and IVIM, for staging LF greater than F2. These results may be credited to the ability of DDC in capturing a continuous distribution of diffusion coefficients from every diffusion compartment (decided by the “no tissue compartmentalization” assumption)<sup>[54,55]</sup>. Beside different diffusion techniques, magnetic resonance elastography (MRE) has also been utilized in many studies for LF staging<sup>[8,25,56]</sup>. Although MRE demonstrated excellent diagnostic ability, even greater than DWI or IVIM, it is currently not widely available around the world since it requires special equipment as well as technical expertise for data acquisition and image postprocessing. However, IVIM is an easy-to-perform and relatively informative technique, which is more widely used in current clinical work.

We acknowledge some limitations in this study. First, although we used QUADAS-2 scale to ensure the high quality of included studies, there were still some studies with retrospective design and unclear blinding method in interpreting IVIM or pathological results, which may introduce inevitable bias and non-objective interpretation of results. Second, substantial heterogeneity was detected in the pooled estimates of LF ≥ F2, therefore we performed subgroup analysis in terms of study design, IVIM protocol *etc.* to explore the potential contributors and used random effects model to summarize our data. However, due to limited eligible studies (less than 10 studies), we did not perform meta-regression to find heterogeneity sources in a significant statistical way. Third, the number of included studies in LF ≥ F1, F3 and F4 was too limited to be further assessed, but the reliability of our results has been confirmed by sensitivity analyses and we believe that should be valuable in clinical



**Table 3** Diagnostic raw data of intravoxel incoherent motion in each liver fibrosis group

Study	Index	Threshold <sup>1</sup>	TP	FP	FN	TN	SEN	SPE
LF ≥ F1								
Chen <i>et al</i> <sup>[24]</sup> , 2014	D*	17.52	20	7	5	18	0.80	0.72
Fu <i>et al</i> <sup>[25]</sup> , 2019	Dt	0.63	75	3	24	23	0.76	0.88
Ichikawa <i>et al</i> <sup>[26]</sup> , 2015	D*	72.15	96	10	14	62	0.87	0.86
Parente <i>et al</i> <sup>[28]</sup> , 2015	D*	37.75	10	13	6	30	0.63	0.70
Wu <i>et al</i> <sup>[27]</sup> , 2015	D*	51.30	27	0	16	6	0.63	1.00
LF ≥ F2								
Fu <i>et al</i> <sup>[25]</sup> , 2019	Dt	0.62	64	7	18	36	0.78	0.84
Hu <i>et al</i> <sup>[29]</sup> , 2017	D*	32.10	30	8	1	17	0.97	0.68
Ichikawa <i>et al</i> <sup>[26]</sup> , 2015	D*	71.72	91	14	6	71	0.94	0.84
Sandrasegaran <i>et al</i> <sup>[32]</sup> , 2018	D*	23.40	31	4	6	8	0.84	0.67
Seo <i>et al</i> <sup>[31]</sup> , 2018	D*	77.64	44	17	7	27	0.86	0.61
Wu <i>et al</i> <sup>[27]</sup> , 2015	D*	40.90	16	3	11	19	0.59	0.86
Yoon <i>et al</i> <sup>[33]</sup> , 2014	D*	43.33	31	0	6	18	0.84	1.00
Yoon <i>et al</i> <sup>[30]</sup> , 2019	D*	70.70	67	2	20	17	0.77	0.89
Zawada <i>et al</i> <sup>[34]</sup> , 2019	Dt	1.00	7	5	7	21	0.50	0.81
LF ≥ F3								
Chung <i>et al</i> <sup>[35]</sup> , 2015	f	0.28	20	5	9	23	0.69	0.82
Fu <i>et al</i> <sup>[25]</sup> , 2019	Dt	0.58	40	16	9	60	0.82	0.79
Ichikawa <i>et al</i> <sup>[26]</sup> , 2015	D*	65.04	78	14	5	85	0.94	0.86
Wu <i>et al</i> <sup>[27]</sup> , 2015	D*	40.90	13	6	4	26	0.76	0.81
LF = F4								
Fu <i>et al</i> <sup>[25]</sup> , 2019	Dt	0.58	23	31	1	70	0.96	0.69
Hu <i>et al</i> <sup>[29]</sup> , 2017	D*	14.44	8	3	2	43	0.80	0.93
Ichikawa <i>et al</i> <sup>[26]</sup> , 2015	D*	61.97	58	24	6	94	0.91	0.80
Seo <i>et al</i> <sup>[31]</sup> , 2018	D*	54.42	22	17	7	49	0.76	0.74
Wu <i>et al</i> <sup>[27]</sup> , 2015	D*	40.30	7	15	0	27	1.00	0.64
Yoon <i>et al</i> <sup>[33]</sup> , 2014	D*	44.17	21	12	0	22	1.00	0.65

<sup>1</sup>The unit of Dt and D\* is 10<sup>-3</sup> mm<sup>2</sup>/s. LF: Liver fibrosis; TP: True positive; FP: False positive; FN: False negative; TN: True negative; SEN: Sensitivity; SPE: Specificity; Dt: True diffusion coefficient; D\*: Pseudo-diffusion coefficient; f: Perfusion fraction.

practice. In the future, more studies are needed to update this meta-analysis for more comprehensive evaluation.

In conclusion, with a larger sample size and the comprehensive statistical analysis, our meta-analysis showed that IVIM is a good diagnostic tool in detecting and staging LF and may serve as a noninvasive substitute to liver biopsy. Moreover, establishing an optimized and standardized IVIM protocol for LF detection and staging would be one of the future directions for its widespread application in patient care.

**Table 4** Summary diagnostic performance and subgroup analysis

Characteristics	No.	Sensitivity	Specificity	Positive LR	Negative LR	DOR	AUC
LF ≥ F1	5	0.78 (0.73-0.82)	0.81 (0.74-0.86)	3.93 (2.12-7.27)	0.30 (0.19-0.46)	15.37 (5.74-41.16)	0.862 (0.811-0.914)
LF ≥ F2	9	0.82 (0.79-0.86)	0.80 (0.75-0.84)	3.69 (2.53-5.37)	0.24 (0.16-0.37)	19.35 (9.51-39.34)	0.883 (0.856-0.909)
LF ≥ F3	4	0.85 (0.79-0.90)	0.83 (0.77-0.87)	4.70 (3.51-6.28)	0.21 (0.10-0.44)	22.61 (8.24-62.05)	0.886 (0.865-0.907)
LF = F4	6	0.90 (0.84-0.94)	0.75 (0.70-0.79)	3.36 (2.57-4.38)	0.16 (0.08-0.31)	26.99 (12.88-56.58)	0.899 (0.866-0.932)
Subgroup analysis in LF ≥ F2							
Study design							
Retrospective	6	0.86 (0.82-0.90)	0.78 (0.71-0.83)	3.73 (2.19-6.34)	0.17 (0.10-0.29)	29.82 (11.65-76.32)	0.921 (0.891-0.952)
Prospective	3	0.71 (0.62-0.79)	0.84 (0.74-0.90)	3.97 (2.42-6.52)	0.42 (0.25-0.69)	10.20 (4.30-24.16)	0.905 (0.862-0.948)
Double blindness							
Yes	3	0.80 (0.74-0.85)	0.75 (0.66-0.83)	3.75 (1.69-8.32)	0.25 (0.19-0.33)	15.46 (8.20-29.14)	0.874 (0.848-0.901)
Unclear	6	0.85 (0.80-0.89)	0.82 (0.76-0.87)	3.80 (2.47-5.84)	0.22 (0.10-0.49)	22.39 (6.91-72.51)	0.892 (0.855-0.930)
Field strength							
1.5 T	3	0.76 (0.68-0.83)	0.81 (0.68-0.90)	3.16 (1.67-5.99)	0.34 (0.18-0.64)	10.40 (3.51-30.87)	0.839 (0.758-0.919)
3.0 T	6	0.85 (0.81-0.89)	0.79 (0.74-0.84)	3.92 (2.42-6.37)	0.19 (0.10-0.36)	26.17 (10.81-63.36)	0.904 (0.872-0.935)
Low b-values (0-50 s/mm <sup>2</sup> )							
< 2	5	0.81 (0.75-0.86)	0.81 (0.73-0.87)	3.40 (2.17-5.35)	0.26 (0.14-0.47)	17.12 (6.11-47.98)	0.877 (0.834-0.921)
≥ 2	4	0.83 (0.78-0.88)	0.79 (0.72-0.85)	4.11 (2.07-8.17)	0.22 (0.10-0.47)	21.73 (7.22-65.42)	0.890 (0.855-0.935)
Trigger method							
RT	5	0.82 (0.77-0.86)	0.79 (0.73-0.84)	3.66 (2.24-5.97)	0.27 (0.14-0.54)	15.05 (5.78-39.22)	0.867 (0.828-0.905)
Non-RT	4	0.83 (0.77-0.88)	0.81 (0.70-0.89)	4.02 (1.85-8.76)	0.21 (0.13-0.34)	29.43 (9.89-87.59)	0.919 (0.883-0.956)

No.: Number of studies; LR: Likelihood ratio; DOR: Diagnostic odds ratio; AUC: Area under summary receiver operating characteristic curves; RT: Respiratory triggered.

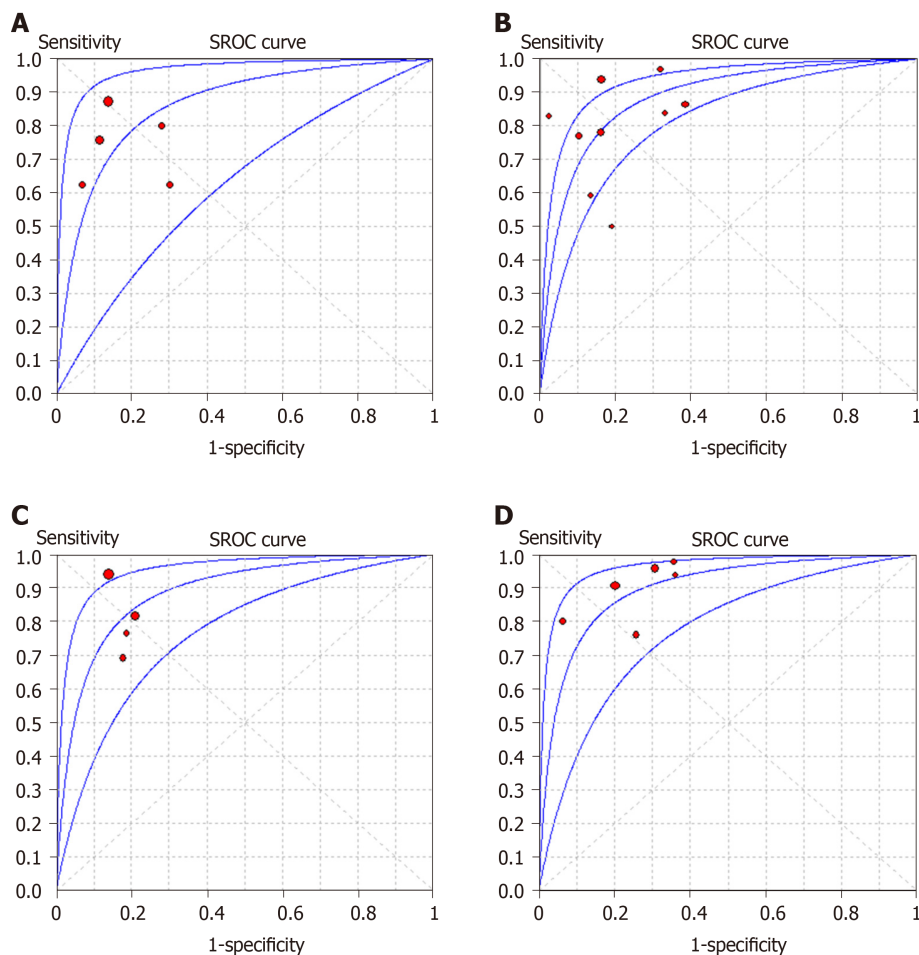


**Figure 3** Summary receiver operating characteristic curves of intravoxel incoherent motion in detecting and staging liver fibrosis. A and B: The area under the curves are 0.862 for liver fibrosis (LF)  $\geq$  F1 (A), B: 0.883 (0.856-0.909) for LF  $\geq$  F2 (B); C and D: 0.886 (0.865-0.907) for LF  $\geq$  F3 (C) and 0.899 (0.866-0.932) for LF = F4 (D), respectively. SROC: Summary receiver operating characteristic.

## ARTICLE HIGHLIGHTS

### Research background

Liver fibrosis (LF) is a common pathological feature of all chronic liver diseases. Liver biopsy is the current reference standard in detecting and staging LF. However, liver biopsy is invasive, observer dependent, and prone to sampling variability, all of which hampers its widespread use in clinical practice; thus, a noninvasive method to quantify LF is urgently needed. Recently, magnetic resonance imaging techniques have been increasingly applied to LF detection and staging and could possibly be the noninvasive alternative to liver biopsy. With the accumulation of extracellular matrix in the fibrotic liver, the true molecular water diffusion and perfusion-related diffusion would be restricted. Intravoxel incoherent motion (IVIM) could capture the information of tissue diffusivity and microcapillary perfusion separately and reflect the fibrotic severity with diffusion coefficients.

### Research motivation

IVIM, a bi-exponential model based on diffusion-weighted imaging, allows for the separate evaluation of true molecular diffusion and perfusion-related diffusion. Although several recent studies focused on the diagnostic performances of IVIM in LF staging, the reported results were discrepant among studies.

### Research objectives

With more eligible studies and patients included, the purpose of this meta-analysis is to investigate the diagnostic performance of IVIM in different LF stages with histology as reference.

### Research methods

A comprehensive literature search was conducted to identify studies on the diagnostic accuracy of IVIM for assessment of histology proven LF. The stages of LF were classified as F0 (no fibrosis), F1 (portal fibrosis without septa), F2 (periportal fibrosis with few septa), F3 (septal fibrosis) and F4 (cirrhosis), according to histopathological findings. Data were extracted to calculate the pooled sensitivity, specificity, positive and negative likelihood ratios and diagnostic

odds ratio, as well as the area under the summary receiver operating characteristic curve (AUC) in each group.

### Research results

Twelve studies with 923 subjects were included in this meta-analysis with 5 studies ( $n = 465$ ) for LF  $\geq$  F1, 9 studies ( $n = 757$ ) for LF  $\geq$  F2, 4 studies ( $n = 413$ ) for LF  $\geq$  F3 and 6 studies ( $n = 562$ ) for LF = F4. The pooled sensitivity and specificity were estimated to be 0.78 (95% confidence interval: 0.73-0.82) and 0.81 (0.74-0.86) for LF  $\geq$  F1 detection with IVIM; 0.82 (0.79-0.86) and 0.80 (0.75-0.84) for staging F2 fibrosis; 0.85 (0.79-0.90) and 0.83 (0.77-0.87) for staging F3 fibrosis, and 0.90 (0.84-0.94) and 0.75 (0.70-0.79) for detecting F4 cirrhosis, respectively. The AUCs for LF  $\geq$  F1, F2, F3, F4 detection were 0.862 (0.811-0.914), 0.883 (0.856-0.909), 0.886 (0.865-0.907) and 0.899 (0.866-0.932), respectively. Moderate to substantial heterogeneity was observed with inconsistency index ( $I^2$ ) ranging from 0% to 77.9%. No publication bias was detected.

### Research conclusions

IVIM is a noninvasive tool with good diagnostic performance in detecting and staging LF. Optimized and standardized IVIM protocols are needed for further improving its diagnostic accuracy in clinical practice.

### Research perspectives

The results showed that IVIM is a valuable tool in noninvasively detecting and staging LF. However, field strength, the number and distribution of b-values, as well as the triggering methods would affect the diagnostic accuracy. There is still a need to establish an optimized and standardized IVIM protocol for LF diagnosis in clinical practice.

## REFERENCES

- 1 Parola M, Pinzani M. Liver fibrosis: Pathophysiology, pathogenetic targets and clinical issues. *Mol Aspects Med* 2019; **65**: 37-55 [PMID: 30213667 DOI: 10.1016/j.mam.2018.09.002]
- 2 Friedman SL. Liver fibrosis -- from bench to bedside. *J Hepatol* 2003; **38** Suppl 1: S38-S53 [PMID: 12591185 DOI: 10.1016/s0168-8278(02)00429-4]
- 3 Trautwein C, Friedman SL, Schuppan D, Pinzani M. Hepatic fibrosis: Concept to treatment. *J Hepatol* 2015; **62**: S15-S24 [PMID: 25920084 DOI: 10.1016/j.jhep.2015.02.039]
- 4 Goodman ZD. Grading and staging systems for inflammation and fibrosis in chronic liver diseases. *J Hepatol* 2007; **47**: 598-607 [PMID: 17692984 DOI: 10.1016/j.jhep.2007.07.006]
- 5 Bedossa P, Dargère D, Paradis V. Sampling variability of liver fibrosis in chronic hepatitis C. *Hepatology* 2003; **38**: 1449-1457 [PMID: 14647056 DOI: 10.1016/j.hep.2003.09.022]
- 6 Martínez SM, Crespo G, Navasa M, Fornis X. Noninvasive assessment of liver fibrosis. *Hepatology* 2011; **53**: 325-335 [PMID: 21254180 DOI: 10.1002/hep.24013]
- 7 Jiang H, Chen J, Gao R, Huang Z, Wu M, Song B. Liver fibrosis staging with diffusion-weighted imaging: a systematic review and meta-analysis. *Abdom Radiol (NY)* 2017; **42**: 490-501 [PMID: 27678393 DOI: 10.1007/s00261-016-0913-6]
- 8 Wang QB, Zhu H, Liu HL, Zhang B. Performance of magnetic resonance elastography and diffusion-weighted imaging for the staging of hepatic fibrosis: A meta-analysis. *Hepatology* 2012; **56**: 239-247 [PMID: 22278368 DOI: 10.1002/hep.25610]
- 9 Besheer T, Elalfy H, Abd El-Maksoud M, Abd El-Razek A, Taman S, Zalata K, Elkashef W, Zaghoul H, Elshahawy H, Raafat D, Elemshaty W, Elsayed E, El-Gilany AH, El-Bendary M. Diffusion-weighted magnetic resonance imaging and micro-RNA in the diagnosis of hepatic fibrosis in chronic hepatitis C virus. *World J Gastroenterol* 2019; **25**: 1366-1377 [PMID: 30918429 DOI: 10.3748/wjg.v25.i11.1366]
- 10 Le Bihan D. What can we see with IVIM MRI? *Neuroimage* 2019; **187**: 56-67 [PMID: 29277647 DOI: 10.1016/j.neuroimage.2017.12.062]
- 11 Le Bihan D, Breton E, Lallemand D, Grenier P, Cabanis E, Laval-Jeantet M. MR imaging of intravoxel incoherent motions: application to diffusion and perfusion in neurologic disorders. *Radiology* 1986; **161**: 401-407 [PMID: 3763909 DOI: 10.1148/radiology.161.2.3763909]
- 12 Tosun M, Onal T, Uslu H, Alparlan B, Çetin Akhan S. Intravoxel incoherent motion imaging for diagnosing and staging the liver fibrosis and inflammation. *Abdom Radiol (NY)* 2020; **45**: 15-23 [PMID: 31705248 DOI: 10.1007/s00261-019-02300-z]
- 13 Huang H, Che-Nordin N, Wang LF, Xiao BH, Chevallier O, Yun YX, Guo SW, Wang YXJ. High performance of intravoxel incoherent motion diffusion MRI in detecting viral hepatitis-b induced liver fibrosis. *Ann Transl Med* 2019; **7**: 39 [PMID: 30906743 DOI: 10.21037/atm.2018.12.33]
- 14 Shin HJ, Yoon H, Kim MJ, Han SJ, Koh H, Kim S, Lee MJ. Liver intravoxel incoherent motion diffusion-weighted imaging for the assessment of hepatic steatosis and fibrosis in children. *World J Gastroenterol* 2018; **24**: 3013-3020 [PMID: 30038468 DOI: 10.3748/wjg.v24.i27.3013]
- 15 França M, Marti-Bonmati L, Alberich-Bayarri A, Oliveira P, Guimaraes S, Oliveira J, Amorim J, Gonzalez JS, Vizcaino JR, Miranda HP. Evaluation of fibrosis and inflammation in diffuse liver diseases using intravoxel incoherent motion diffusion-weighted MR imaging. *Abdom Radiol (NY)* 2017; **42**: 468-477 [PMID: 27638516 DOI: 10.1007/s00261-016-0899-0]
- 16 Zhang B, Liang L, Dong Y, Lian Z, Chen W, Liang C, Zhang S. Intravoxel Incoherent Motion MR Imaging for Staging of Hepatic Fibrosis. *PLoS One* 2016; **11**: e0147789 [PMID: 26820668 DOI: 10.1371/journal.pone.0147789]
- 17 Whiting PF, Rutjes AW, Westwood ME, Mallett S, Deeks JJ, Reitsma JB, Leeflang MM, Sterne JA, Bossuyt PM; QUADAS-2 Group. QUADAS-2: a revised tool for the quality assessment of diagnostic accuracy studies. *Ann Intern Med* 2011; **155**: 529-536 [PMID: 22007046 DOI: 10.7326/0003-4819-155-8-201110180-00009]
- 18 Vamvakas EC. Meta-analyses of studies of the diagnostic accuracy of laboratory tests: a review of the concepts and methods. *Arch Pathol Lab Med* 1998; **122**: 675-686 [PMID: 9701328]
- 19 Moses LE, Shapiro D, Littenberg B. Combining independent studies of a diagnostic test into a summary

- ROC curve: data-analytic approaches and some additional considerations. *Stat Med* 1993; **12**: 1293-1316 [PMID: 8210827 DOI: 10.1002/sim.4780121403]
- 20 **Higgins JP**, Thompson SG. Quantifying heterogeneity in a meta-analysis. *Stat Med* 2002; **21**: 1539-1558 [PMID: 12111919 DOI: 10.1002/sim.1186]
- 21 **Zamora J**, Abraira V, Muriel A, Khan K, Coomarasamy A. Meta-DiSc: a software for meta-analysis of test accuracy data. *BMC Med Res Methodol* 2006; **6**: 31 [PMID: 16836745 DOI: 10.1186/1471-2288-6-31]
- 22 **Macaskill P**, Gatsonis C, Deeks J, Harbord R, Takwoingi Y. Chapter 10 Analysing and Presenting Results, Cochrane Handbook for Systematic Reviews of Diagnostic Test Accuracy Version 1.0. The Cochrane Collaboration. 2010. Available from: <https://methods.cochrane.org/sites/methods.cochrane.org.sdt/files/public/uploads/Chapter%2010%20-%20Version%201.0.pdf>
- 23 **Deeks JJ**, Macaskill P, Irwig L. The performance of tests of publication bias and other sample size effects in systematic reviews of diagnostic test accuracy was assessed. *J Clin Epidemiol* 2005; **58**: 882-893 [PMID: 16085191 DOI: 10.1016/j.jclinepi.2005.01.016]
- 24 **Chen C**, Wang B, Shi D, Fu F, Zhang J, Wen Z, Zhu S, Xu J, Lin Q, Li J, Dou S. Initial study of biexponential model of intravoxel incoherent motion magnetic resonance imaging in evaluation of the liver fibrosis. *Chin Med J (Engl)* 2014; **127**: 3082-3087 [PMID: 25189949]
- 25 **Fu F**, Li X, Chen C, Bai Y, Liu Q, Shi D, Sang J, Wang K, Wang M. Non-invasive assessment of hepatic fibrosis: comparison of MR elastography to transient elastography and intravoxel incoherent motion diffusion-weighted MRI. *Abdom Radiol (NY)* 2020; **45**: 73-82 [PMID: 31372777 DOI: 10.1007/s00261-019-02140-x]
- 26 **Ichikawa S**, Motosugi U, Morisaka H, Sano K, Ichikawa T, Enomoto N, Matsuda M, Fujii H, Onishi H. MRI-based staging of hepatic fibrosis: Comparison of intravoxel incoherent motion diffusion-weighted imaging with magnetic resonance elastography. *J Magn Reson Imaging* 2015; **42**: 204-210 [PMID: 25223820 DOI: 10.1002/jmri.24760]
- 27 **Wu CH**, Ho MC, Jeng YM, Liang PC, Hu RH, Lai HS, Shih TT. Assessing hepatic fibrosis: comparing the intravoxel incoherent motion in MRI with acoustic radiation force impulse imaging in US. *Eur Radiol* 2015; **25**: 3552-3559 [PMID: 25991478 DOI: 10.1007/s00330-015-3774-4]
- 28 **Parente DB**, Paiva FF, Oliveira Neto JA, Machado-Silva L, Figueiredo FA, Lanzoni V, Campos CF, do Brasil PE, Gomes Mde B, Perez Rde M, Rodrigues RS. Intravoxel Incoherent Motion Diffusion Weighted MR Imaging at 3.0 T: Assessment of Steatohepatitis and Fibrosis Compared with Liver Biopsy in Type 2 Diabetic Patients. *PLoS One* 2015; **10**: e0125653 [PMID: 25961735 DOI: 10.1371/journal.pone.0125653]
- 29 **Hu F**, Yang R, Huang Z, Wang M, Zhang H, Yan X, Song B. Liver fibrosis: in vivo evaluation using intravoxel incoherent motion-derived histogram metrics with histopathologic findings at 3.0 T. *Abdom Radiol (NY)* 2017; **42**: 2855-2863 [PMID: 28624925 DOI: 10.1007/s00261-017-1208-2]
- 30 **Yoon JH**, Lee JM, Lee KB, Kim D, Kabasawa H, Han JK. Comparison of monoexponential, intravoxel incoherent motion diffusion-weighted imaging and diffusion kurtosis imaging for assessment of hepatic fibrosis. *Acta Radiol* 2019; **60**: 1593-1601 [PMID: 30935212 DOI: 10.1177/0284185119840219]
- 31 **Seo N**, Chung YE, Park YN, Kim E, Hwang J, Kim MJ. Liver fibrosis: stretched exponential model outperforms mono-exponential and bi-exponential models of diffusion-weighted MRI. *Eur Radiol* 2018; **28**: 2812-2822 [PMID: 29404771 DOI: 10.1007/s00330-017-5292-z]
- 32 **Sandrasegaran K**, Territo P, Elkady RM, Lin Y, Gasparis P, Borthakur G, Lin C. Does intravoxel incoherent motion reliably stage hepatic fibrosis, steatosis, and inflammation? *Abdom Radiol (NY)* 2018; **43**: 600-606 [PMID: 28828711 DOI: 10.1007/s00261-017-1263-8]
- 33 **Yoon JH**, Lee JM, Baek JH, Shin CI, Kiefer B, Han JK, Choi BI. Evaluation of hepatic fibrosis using intravoxel incoherent motion in diffusion-weighted liver MRI. *J Comput Assist Tomogr* 2014; **38**: 110-116 [PMID: 24378888 DOI: 10.1097/RCT.0b013e3182a589be]
- 34 **Zawada E**, Serafin Z, Dybowska D, Halota W, Wypych A, Nadolska K, Rusak G. Monoexponential and Biexponential Fitting of Diffusional Magnetic Resonance Imaging Signal Analysis for Prediction of Liver Fibrosis Severity. *J Comput Assist Tomogr* 2019; **43**: 857-862 [PMID: 31738209 DOI: 10.1097/RCT.0000000000000937]
- 35 **Chung SR**, Lee SS, Kim N, Yu ES, Kim E, Kühn B, Kim IS. Intravoxel incoherent motion MRI for liver fibrosis assessment: a pilot study. *Acta Radiol* 2015; **56**: 1428-1436 [PMID: 25414372 DOI: 10.1177/0284185114559763]
- 36 **Wáng YXJ**. Living tissue intravoxel incoherent motion (IVIM) diffusion MR analysis without  $b=0$  image: an example for liver fibrosis evaluation. *Quant Imaging Med Surg* 2019; **9**: 127-133 [PMID: 30976535 DOI: 10.21037/qims.2019.01.07]
- 37 **Li YT**, Cercueil JP, Yuan J, Chen W, Löffroy R, Wáng YX. Liver intravoxel incoherent motion (IVIM) magnetic resonance imaging: a comprehensive review of published data on normal values and applications for fibrosis and tumor evaluation. *Quant Imaging Med Surg* 2017; **7**: 59-78 [PMID: 28275560 DOI: 10.21037/qims.2017.02.03]
- 38 **Luciani A**, Vignaud A, Cavet M, Nhieu JT, Mallat A, Ruel L, Laurent A, Deux JF, Brugieres P, Rahmouni A. Liver cirrhosis: intravoxel incoherent motion MR imaging--pilot study. *Radiology* 2008; **249**: 891-899 [PMID: 19011186 DOI: 10.1148/radiol.2493080080]
- 39 **Dyvorne HA**, Galea N, Nevers T, Fiel MI, Carpenter D, Wong E, Orton M, de Oliveira A, Feiweier T, Vachon ML, Babb JS, Taouli B. Diffusion-weighted imaging of the liver with multiple b values: effect of diffusion gradient polarity and breathing acquisition on image quality and intravoxel incoherent motion parameters--a pilot study. *Radiology* 2013; **266**: 920-929 [PMID: 23220895 DOI: 10.1148/radiol.12120686]
- 40 **ter Voert EE**, Delso G, Porto M, Huellner M, Veit-Haibach P. Intravoxel Incoherent Motion Protocol Evaluation and Data Quality in Normal and Malignant Liver Tissue and Comparison to the Literature. *Invest Radiol* 2016; **51**: 90-99 [PMID: 26405835 DOI: 10.1097/RLL.0000000000000207]
- 41 **Cohen AD**, Schieke MC, Hohenwarter MD, Schmainda KM. The effect of low b-values on the intravoxel incoherent motion derived pseudodiffusion parameter in liver. *Magn Reson Med* 2015; **73**: 306-311 [PMID: 24478175 DOI: 10.1002/mrm.25109]
- 42 **Wáng YXJ**, Li YT, Chevallier O, Huang H, Leung JCS, Chen W, Lu PX. Dependence of intravoxel incoherent motion diffusion MR threshold b-value selection for separating perfusion and diffusion compartments and liver fibrosis diagnostic performance. *Acta Radiol* 2019; **60**: 3-12 [PMID: 29742916 DOI: 10.1177/0284185118774913]
- 43 **Dyvorne H**, Jajamovich G, Kakite S, Kuehn B, Taouli B. Intravoxel incoherent motion diffusion imaging of the liver: optimal b-value subsampling and impact on parameter precision and reproducibility. *Eur J*

- Radiol* 2014; **83**: 2109-2113 [PMID: 25277521 DOI: 10.1016/j.ejrad.2014.09.003]
- 44 **Lee Y**, Lee SS, Kim N, Kim E, Kim YJ, Yun SC, Kühn B, Kim IS, Park SH, Kim SY, Lee MG. Intravoxel incoherent motion diffusion-weighted MR imaging of the liver: effect of triggering methods on regional variability and measurement repeatability of quantitative parameters. *Radiology* 2015; **274**: 405-415 [PMID: 25232802 DOI: 10.1148/radiol.14140759]
- 45 **Jerome NP**, Orton MR, d'Arcy JA, Collins DJ, Koh DM, Leach MO. Comparison of free-breathing with navigator-controlled acquisition regimes in abdominal diffusion-weighted magnetic resonance images: Effect on ADC and IVIM statistics. *J Magn Reson Imaging* 2014; **39**: 235-240 [PMID: 23580454 DOI: 10.1002/jmri.24140]
- 46 **Shan Y**, Zeng MS, Liu K, Miao XY, Lin J, Fu Cx, Xu PJ. Comparison of Free-Breathing With Navigator-Triggered Technique in Diffusion Weighted Imaging for Evaluation of Small Hepatocellular Carcinoma: Effect on Image Quality and Intravoxel Incoherent Motion Parameters. *J Comput Assist Tomogr* 2015; **39**: 709-715 [PMID: 26196345 DOI: 10.1097/RCT.0000000000000278]
- 47 **Leporq B**, Saint-Jalmes H, Rabrait C, Pilleul F, Guillaud O, Dumortier J, Scoazec JY, Beuf O. Optimization of intra-voxel incoherent motion imaging at 3.0 Tesla for fast liver examination. *J Magn Reson Imaging* 2015; **41**: 1209-1217 [PMID: 25044653 DOI: 10.1002/jmri.24693]
- 48 **Riexinger AJ**, Martin J, Rauh S, Wetscherek A, Pistel M, Kuder TA, Nagel AM, Uder M, Hensel B, Müller L, Laun FB. On the Field Strength Dependence of Bi- and Triexponential Intravoxel Incoherent Motion (IVIM) Parameters in the Liver. *J Magn Reson Imaging* 2019; **50**: 1883-1892 [PMID: 30941806 DOI: 10.1002/jmri.26730]
- 49 **Cui Y**, Dyvorne H, Besa C, Cooper N, Taouli B. IVIM Diffusion-weighted Imaging of the Liver at 3.0T: Comparison with 1.5T. *Eur J Radiol Open* 2015; **2**: 123-128 [PMID: 26393236 DOI: 10.1016/j.ejro.2015.08.001]
- 50 **Yang L**, Rao S, Wang W, Chen C, Ding Y, Yang C, Grimm R, Yan X, Fu C, Zeng M. Staging liver fibrosis with DWI: is there an added value for diffusion kurtosis imaging? *Eur Radiol* 2018; **28**: 3041-3049 [PMID: 29383522 DOI: 10.1007/s00330-017-5245-6]
- 51 **Tosun M**, Inan N, Sarisoy HT, Akansel G, Gumustas S, Gürbüz Y, Demirci A. Diagnostic performance of conventional diffusion weighted imaging and diffusion tensor imaging for the liver fibrosis and inflammation. *Eur J Radiol* 2013; **82**: 203-207 [PMID: 23122674 DOI: 10.1016/j.ejrad.2012.09.009]
- 52 **Cercueil JP**, Petit JM, Nougaret S, Soyer P, Fohlen A, Pierredon-Foulongne MA, Schembri V, Delhom E, Schmidt S, Denys A, Aho S, Guiu B. Intravoxel incoherent motion diffusion-weighted imaging in the liver: comparison of mono-, bi- and tri-exponential modelling at 3.0-T. *Eur Radiol* 2015; **25**: 1541-1550 [PMID: 25527431 DOI: 10.1007/s00330-014-3554-6]
- 53 **Fu F**, Shi D, Zhu S, Wang M, Chen C, Li D, Li J, Dou S. Evaluation of hepatic fibrosis by using stretched-exponential and mono-exponential diffusion-weighted MR imaging. *Int J Clin Exp Med* 2016; **9**: 21358-21367
- 54 **Bennett KM**, Schmainda KM, Bennett RT, Rowe DB, Lu H, Hyde JS. Characterization of continuously distributed cortical water diffusion rates with a stretched-exponential model. *Magn Reson Med* 2003; **50**: 727-734 [PMID: 14523958 DOI: 10.1002/mrm.10581]
- 55 **Anderson SW**, Barry B, Soto J, Ozonoff A, O'Brien M, Jara H. Characterizing non-gaussian, high b-value diffusion in liver fibrosis: Stretched exponential and diffusional kurtosis modeling. *J Magn Reson Imaging* 2014; **39**: 827-834 [PMID: 24259401 DOI: 10.1002/jmri.24234]
- 56 **Hennedige TP**, Wang G, Leung FP, Alsaif HS, Teo LL, Lim SG, Wee A, Venkatesh SK. Magnetic Resonance Elastography and Diffusion Weighted Imaging in the Evaluation of Hepatic Fibrosis in Chronic Hepatitis B. *Gut Liver* 2017; **11**: 401-408 [PMID: 27965475 DOI: 10.5009/gnl16079]



Published by Baishideng Publishing Group Inc  
7041 Koll Center Parkway, Suite 160, Pleasanton, CA 94566, USA  
Telephone: +1-925-3991568  
E-mail: [bpgoffice@wjgnet.com](mailto:bpgoffice@wjgnet.com)  
Help Desk: <http://www.f6publishing.com/helpdesk>  
<http://www.wjgnet.com>

